

## Research article

---

# A Novel Method Using Two-stage Anaerobic Digestion Integrated with Greenhouse Solar Dryer for Increased Biogas Production

Thaithat Sudsuansee\*, Wanrop Khanthirat, Amin Lawong and Supakit Sergsiri

*Division of Industrial Engineering, Faculty of Engineering and Industrial Technology, Kalasin University, Kalasin, Thailand*

Received: 27 June 2022, Revised: 30 August 2022, Accepted: 10 January 2023

DOI: 10.55003/cast.2023.05.23.002

## Abstract

### Keywords

anaerobic digestion;  
biogas;  
greenhouse solar dryer;  
solar energy

Solar energy is infinite and environmental-friendly energy that is widely used in many fields such as solar cells, solar roofs, solar dryers and so on. However, solar energy has never been used in anaerobic digestion processes for biogas production. The use of solar energy may accelerate the biogas reaction to achieve higher gas production rates. Hence, the purpose of this research was to study a two-stage anaerobic digestion system in combination with a greenhouse solar dryer to increase the rate of biogas production. The study consisted of two parts: the first was to study the temperature variations in greenhouse solar dryers using computational fluid dynamic techniques, and the second was to conduct two-stage anaerobic digestion integrated with the greenhouse solar dryer system for biogas production. The results showed that the average temperature and biogas production rate in the integrated two-stage anaerobic digestion system compared to a conventional system increased by 16.2% and 19.69 %, respectively.

## 1. Introduction

The two-stage anaerobic digestion (TSAD) process to produce biogas is an important process in the disposal of bio-waste. TSAD used for the biodegradation process is extremely efficient and offers the advantages of low cost and low emission generation [1]. It has also good system stability and high biogas production rates. This is because the system is designed to provide specific conditions for both the acidification and metagenesis digestion stages. An important factor affecting the efficiency of the TSAD process is the temperature of the system. A literature review found that temperature control in the thermophilic range (50-60°C) made the digestion system more efficient than it was in the mesophilic range (30-40°C) [2]. However, if the system temperature is too high, the system consumes a high amount of energy, making it difficult to control the system, and

---

\*Corresponding author: Tel.: (+66) 915166444  
E-mail: thaithat.su@ksu.ac.th

increasing the risk of system failure. Past research has shown that controlling the system temperature at approximately 38°C results in higher system efficiency, higher biogas production, and lower production costs [3]. Thailand is a country that has sunlight all year round, and solar energy is a clean and inexhaustible energy source. Therefore, it is appropriate that solar energy should be used for heating applications such as digestion systems where its use can increase biogas production performance. Considering the average ambient temperature in Thailand is 28°C [4], it is sensible to increase the digestion temperature with the solar heating technology known as a greenhouse solar dryer (GSD) in order to keep the process in the mesophilic temperature range, and thus improve the TSAD process. This was the main aim of this research, and more details are described in the next section.

A greenhouse solar dryer (GSD) used for a drying technology process, is widely used in Thailand [5]. It is mostly utilized in food drying operations; however, it can also be employed in heating processes for other applications. Its structure resembles a parabolic shape with a roof made of polycarbonate material. The working principle starts with the radiation emitted by the sun shining through the GSD roof surface and hitting the ground inside, where the radiation is reflected or absorbed. Some of the reflected heat is trapped under the GSD roof surface, causing the temperature inside the GSD to increase due to the greenhouse effect. When the internal temperature exceeds the set value, the temperature controller installed in the system begins to operate and maintains the temperature by sending a signal to the control device or fan used to reduce the temperature by exhausting hot air to the outside. An experimental study of tomato drying using a GSD [5] found that dehydrated tomatoes could be produced at up to 1,000 kg each time using a GSD of area 160 m<sup>2</sup> with a height of 3.5 m. GSD can also dry a wide variety of products such as fruits and vegetables, herbs and spices, rice and grain products, coffee beans, and tea leaves [5].

Among the benefits of GSD is its ability to increase and maintain temperature effectively. This led to the idea of using a GSD in a TSAD process, which was unprecedented. The use of a GSD integrated into a TSAD system can increase digestion temperature within the mesophilic range (30-40°C). In general, one obstacle to maintaining a temperature within the GSD is the variation in temperature during the day. Typically, temperatures begin to rise in the morning, peak in the afternoon, and decrease steadily at night. When the system temperature is above 40°C, a thermostat activates an exhaust fan to cool the GSD, keeping the internal temperature levels close to the setting value. On the other hand, at night, the temperature outside the system is lower than inside, and system heat loss occurs. But it is relatively small because the internal greenhouse effect causes the system to decrease temperature gradually and the temperature value does not go too low. The average daily temperature of a TSAD system with GSD tends to be higher than that without a GSD system, which may result in the increase of biogas production rate and overall TSAD system efficiency.

This research was aimed at increasing the average temperature within a TSAD system by integrating it with a GSD. The research steps were as follows: 1) analysis of temperature variations within the GSD throughout the day using computational fluid dynamics (CFD) software, 2) development of a GSD based on TSAD system, and 3) comparison of the biogas production rates of a TSAD systems with GSD and a traditional systems (GSD-free). The researchers expect that this research will be applied at the community level in the future.

## 2. Materials and Methods

### 2.1 Solar radiation

#### 2.1.1 Clear-sky solar radiation

The solar radiation radiated in a clear sky is defined as a beam or direct and diffuse. Direct is the radiation sent directly from the sun. Diffuse is the radiation that hits the sky and is diffused onto an object, both of which can be expressed as follows:

$$\begin{aligned} E_b &= E_0 \exp(-\tau_b m^{ab}) \\ E_d &= E_0 \exp(-\tau_d m^{ad}) \end{aligned} \quad (1)$$

where  $E_b$  = direct radiation intensity (measured perpendicular to the sun)  
 $E_d$  = diffuse radiation intensity value (measured on a horizontal surface)  
 $E_0$  = Extraterrestrial Orthogonal Intensity [6]  
 $m$  = air mass [7]

$\tau_b, \tau_d$  = Beam and diffuse optical depths, which depend on the terrain of the area and vary during the year and an average can be obtained from ASHRAE RP-1453 [8].

$ab, ad$  = The direct and diffuse air mass components that are obtained from the equation:

$$\begin{aligned} ab &= 1.219 - 0.043\tau_b - 0.151\tau_d - 0.204\tau_b\tau_d \\ ad &= 0.202 - 0.852\tau_b - 0.007\tau_d - 0.357\tau_b\tau_d \end{aligned} \quad (2)$$

#### 2.1.2 The relation between the solar angle and the receiving surface

Figure 1 shows the orientation of the light-receiving surface. The inclination angle  $\Sigma$  is the angle between the object's surface and the horizontal plane. zenith surface angle  $\psi$  is defined as a reference distance from the south. The azimuth angle between the surface and the sun  $\gamma$  is the value of the angle difference between the solar azimuth angle  $\phi$  and the azimuth surface angle  $\gamma = \phi - \psi$ .

The angle between the perpendicular line to the surface and the earth-sun line is called the angle of incidence  $\theta$ . It is important to calculate the load of solar energy because it affects the intensity of the direct solar radiation acting on the surface and the ability to absorb, transmit or reflect the radiation. Its value is obtained from the equation:

$$\cos \theta = \cos \beta \cos \gamma \sin \Sigma + \sin \beta \cos \Sigma \quad (3)$$

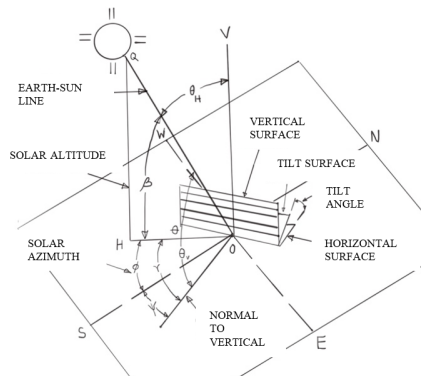


**Figure 1.** Solar angle for vertical and horizontal surfaces [9]

### 2.1.3 Calculation of the incident sunlight intensity on the irradiated surface

The total radiation intensity  $E_t$  acting on the receiving surface is the sum of three components: the beam component  $E_{t,b}$  originating from the sun, the diffuse component  $E_{t,d}$  originating from the horizon, and the ground-reflected radiation component  $E_{t,r}$  originating from the ground in front of the receiving surface.

$$E_t = E_{t,b} + E_{t,d} + E_{t,r} \quad (4)$$

The scattered radiation is obtained from the following relation:

$$E_{t,b} = E_b \cos \theta \quad (5)$$

In which  $\theta$  is the angle of incidence. This relationship is valid when  $\cos \theta > 0$ ; otherwise,  $E_{t,b} = 0$ .

With reference to diffuse radiation in the case of a vertical surface, Stephenson [10] and Threlkeld [11] show that the Y ratio of the vertical surface diffusion intensity to the horizontal surface diffusion intensity is a function of the angle of incidence.

$$E_{t,d} = E_d Y$$

$$Y = \max(0.45, 0.55 + 0.437 \cos \theta + 0.313 \cos^2 \theta) \quad (6)$$

The reflected ray can be defined as

$$E_{t,r} = (E_b \sin \beta + E_d) \rho_g \frac{1 - \cos \Sigma}{2} \quad (7)$$

where  $\rho_g$  is the ground reflectance value of 0.2 for a general mixed surface.

## 2.2 Greenhouse solar dryer (GSD)

The GSD used in this research was developed by Janjai [5]. Its function is drying objects using solar energy as the main power source.

### 2.2.1 Working principle of GSD

The working principle of a GSD relies on the principle of the greenhouse effect, as shown in Figure 2. Solar radiation is transmitted through the ozone layer into the earth's atmosphere at point 1. It consists of various wavelengths. When it reaches the sheet of glass or clear plastic that makes up the roof of GSD, ultraviolet rays (UV) are reflected, as seen point 2. However, short-wavelength solar radiation can pass through the GSD, as shown in point 3. These then incidents upon the material surface within the GSD and are absorbed, as shown at point 4. As a result, shortwave solar radiation is reduced in energy and converted to long-wavelength solar radiation and thermal radiation or infrared radiation. This heat radiation cannot penetrate through the glass or clear plastic to the outside as shown in point 5, and it then heats the temperature inside the greenhouse. Heat is transferred to objects inside the greenhouse as shown in point 6, and water within the objects is evaporated into the air as shown in point 7. High-humidity air is discharged from the GSD by an exhaust fan supplied by a photovoltaic power generation system as shown in point 8. Finally, low temperature and humidity air from outside will be drawn into GSD instead of the high humidity air, as shown at point 9.

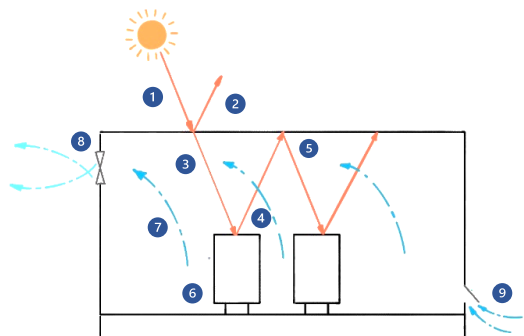


**Figure 2.** Working principle of a GSD

### 2.2.2 Energy and mass balance of GSD

This research used the energy and mass balance of a GSD that was derived by Janjai *et al.* [12], with the assumptions that 1) the air flow is unidirectional and there is no separation of the air layer within the GSD, and 2) the specific heat of the air and that of the GSD is equal.

#### 1) The energy balance of parabolic dome of GSD

The energy balance of parabolic dome of a GSD can be explained by the rate of accumulation of thermal energy inside the parabolic dome, which is equal to the rate of transfer of thermal energy between the air inside and the dome due to convection plus the rate of transfer of thermal energy between the sky and the dome due to radiation plus the rate of transfer of thermal energy between

the dome and the environment due to convection plus the rate of transfer of thermal energy between the digestor and the dome due to radiation plus the rate of radiation absorption by the dome.

The energy balance equation of a parabolic dome [12] is:

$$m_c C_{pc} \frac{dT_c}{dt} = A_c h_{c,c-a} (T_a - T_c) + A_c h_{r,c-s} (T_s - T_c) + A_c h_w (T_{am} - T_c) + A_p h_{r,p-c} (T_p - T_c) + A_c \alpha_c I_t \quad (8)$$

The energy balance equation for air within the GSD [12] is:

$$m_a C_{pa} \frac{dT_a}{dt} = A_p h_{c,p-a} (T_p - T_a) + A_f h_{c,f-a} (T_f - T_a) + D_p A_p C_{pv} \rho_p (T_p - T_a) \frac{dM_p}{dt} + (p_a V_{out} C_{pa} T_{out} - \rho_a V_{in} C_{pa} T_{in}) + U_c A_c (T_{am} - T_a) + [(1 - F_p)(1 - \alpha_f) + (1 - \alpha_p) F_p] I_t A_c \tau_c \quad (9)$$

## 2) Energy balance of digestor

The energy equilibrium can be explained by the rate of thermal energy accumulation in the digestor, which is equal to the rate of heat energy received from the air by the digestor due to convection plus the rate of heat energy transfer between the dome and the digestor due to thermal radiation plus the rate of heat energy loss from the digestor due to latent heat loss plus the rate of absorption of heat energy by the digestor [12].

$$m_p (C_{pp} + C_{pl} M_p) \frac{dT_p}{dt} = A_p h_{c,p-a} (T_a - T_p) + A_p h_{r,p-c} (T_c - T_p) + D_p A_p \rho_p L_p \frac{dM_p}{dt} + F_p \alpha_p I_t A_c \tau_c \quad (10)$$

## 3) Energy balancing on concrete floor

Energy equilibrium can be explained by the rate of accumulation of thermal energy in the floor, which is the rate of heat transfer due to convection between the air in the GSD and the floor plus the rate of thermal conductivity between the concrete floor and the ground plus the rate of absorption of solar thermal radiation on the concrete floor [12].

$$m_f C_{pf} \frac{dT_f}{dt} = A_f h_{c,f-a} (T_a - T_f) + A_f h_{D,f-g} (T_g - T_f) + (1 - F_p) \alpha_f I_t A_f \tau_c \quad (11)$$

## 4) Equation of mass equilibrium

Mass equilibrium can be explained by the rate of accumulation of air moisture within the GSD, which is equal to the rate at which moisture enters the GSD from the outside minus the rate of moisture leaving the GSD due to air outflow plus the rate of moisture loss from the digestor [12].

$$\rho_a V \frac{dH}{dt} = A_{in} \rho_a H_{in} v_{in} - A_{out} \rho_a H_{out} v_{out} + D_p A_p \rho_p \frac{dM_p}{dt} \quad (12)$$

### 2.3 Two-stage anaerobic digestion (TSAD)

In a TSAD system, the operation consists of two stages, acidification, and metagenesis. The separation into a two-stage process enables the specific conditions under which digestion performance can be improved. Figure 3 shows a TSAD system with an acid tank for the stage of acidification and a methane tank for the stage of methanogenesis [13]. Acidification is a combination of acidogenesis and acetogenesis processes. The hydrolyzed organic compounds are bio-transformed into volatile fatty acids (VFAs) in the acidogenesis process and the VFAs and other intermediates formed are converted to acetates and hydrogen in the acetogenesis process [13]. Acidification is a process that takes a short time, and the pH value of the system is 5.0-6.0. In the stage of methanogenesis, acetates are essential substrates that can be directly utilized by methanogens for methane production. At this stage, the system's hydraulic retention time (HRT) is 20-30 days which is longer than the acidification stage and the system's pH value is 6.0-8.0 [14]. The advantages of the TSAD system are high system stability, high organic loading rates (OLR), short HRT times, and high volatile solids (VS) and chemical oxygen demand (COD) removal compared to single-stage AD systems.

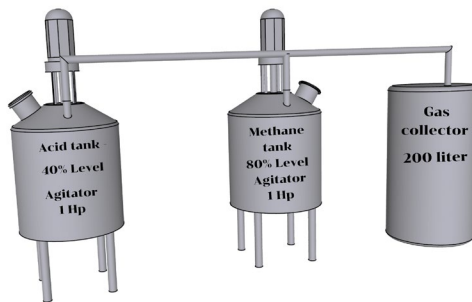


**Figure 3.** TSAD diagram.

### 2.4 Research framework

This research uses a new TSAD system integrated with a GSD to achieve higher biogas production rates. The experiment results of the GSD-integrated system were compared with a GSD-free (traditional) system. The framework for the proposed method is shown in Figure 4.

### 2.5 GSD and GSD-free system characteristics

Figure 5 shows the GSD, a parabolic dome with a diameter of  $6 \times 6$  m and a height of 3 m. At the sides of the dome, there are exhaust fans to ventilate excess heat to the outside and bring cool air inside, preventing the temperature inside the dome from getting too high. The walls are made of polycarbonate, which is a good heat transfer material. Inside the dome, a two-stage anaerobic digester is installed to produce biogas from food waste.

The GSD-integrated system is a biogas digestion system that has a TSAD placed in the GSD. The TSAD system incorporates stainless steel fermentation tanks to effectively transfer heat throughout the system. Additionally, the digester has motorized automatic stirring blades to assist in catalyzing chemical reactions.

The GSD-free system is a typical biogas digestion system with a TSAD housed in a covered structure with effective internal ventilation. PVC fermentation tanks are used in a TSAD, and manual stirring blades are included to assist in catalyzing chemical reactions.

Both experimental systems utilized the same organic waste from the same source and fed it into the system, at the same rate, on the same day, and at the same time.

## 2.6 Analysis of temperature variation within GSD

The first step of the TSAD experiment was to analyze the temperature variations within the system. The temperature change of the system is due to the accumulated heat inside the GSD. Solar radiation is transmitted through the GSD surface and hits the wall of the biogas digester (stainless steel tank), causing heat accumulation and system temperature rise, as shown in Figure 6. The heat at the walls of the digester is conducted to the substance inside the digester, causing the temperature of the substance to rise. This process is analyzed using scSTREAM, a software for thermo-fluid analysis with CFDs. The calculation is based on a structured mesh and grid construction using cut-cell and finite elements techniques, as shown in Figure 7. Fluid analysis is an incompressible turbulent k- $\epsilon$  flow. Solar radiation analysis is based on data from the ASHRAE handbook [9]. Solar radiation values for September 2021 were calculated according to the manual. The position of the GSD system was 16.43 degrees latitude and 102.8 degrees longitude. The experiment was started at 7:00 am and ran onwards for 24 h. The reflectance of the incident solar radiation was 0.5 and the cloud coefficient was set to 0.1.

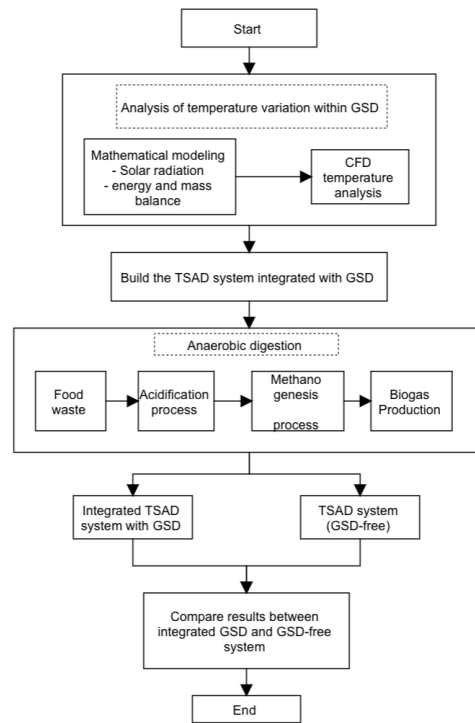


**Figure 4.** The framework for this research



**Figure 5.** Greenhouse solar dryer (GSD)

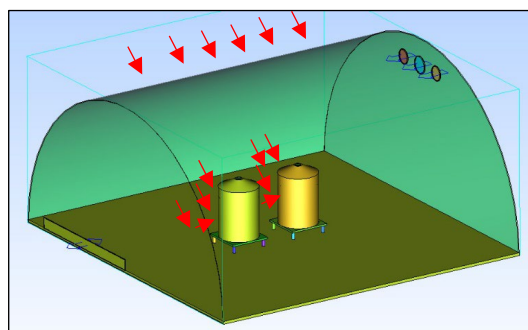


**Figure 6.** Transmitting solar radiation through the GSD system (CFD model)

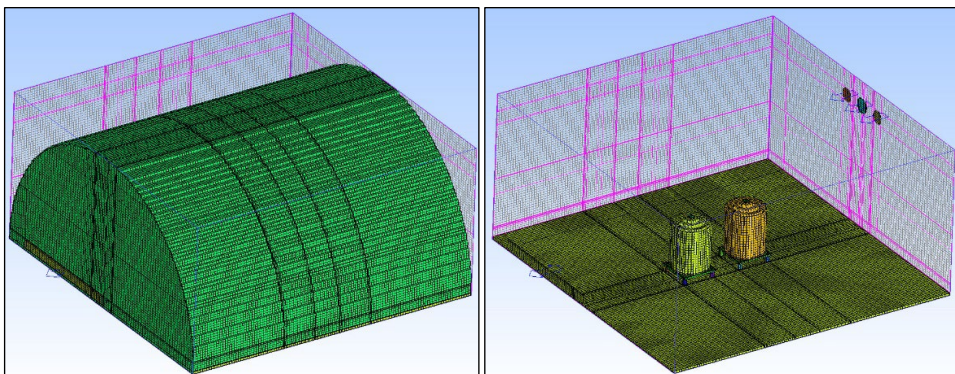


**Figure 7.** A structured mesh and grid construction of an GSD-integrated system (CFD model)

## 2.7 TSAD process

In the first stage of TSAD, cow manure was taken as a substrate (a combination of bio-waste and microorganisms). A 20 kg of cow manure was added to the methane tank, and then water was added at a ratio of 1:1 (20 L). The methane tank was then closed to ferment for about 10 days. After the process was complete, 10 kg of cow manure was added to the acid tank. Then water was added to a volume of 40 L (40% of tank volume), and the tank was closed. Acid production, which took about a day, was then allowed to take place.

In the next step, organic waste from the municipal fresh market was added daily. The non-food waste was separated, and 1 kg of the remaining organic waste was crushed to a size of less than 1 cm to increase the biodegradation reaction rate. After that, water was added to the separated food waste at a ratio of 1:1 to adjust the solids content ratio to approximately 10%. It was then loaded into the acid tank (Figure 8), with an agitator driven by a 1 Hp 220 V motor. Meanwhile, the acid organic waste from the acid tank was semi-continuously loaded into a methane tank, the total volume of which is approximately 80 L. An agitator powered by a 1 Hp 220 V motor circulated the substances in the tank. The hydraulic retention period (HRT) was 24 days. The produced biogas gradually flowed out of the methane tank through the gas pipe into the storage tank. When the biogas volume was constant or the system reached a steady-state, the system operation was stopped.



**Figure 8.** Anaerobic digestion (AD) system

## 2.8 Experimental study of an integrated TSAD system with GSD and a traditional system (GSD-free)

An experimental study of the TSAD system integrated with GSD and GSD-free was performed with the same method described in Section 2.3. The experimental results were compared and analyzed to evaluate the temperature values affecting the biogas production rate. We also conducted experiments to determine other study parameters. In the measurement of parameters, samples were collected and measured three times per experiment. The values obtained in the experiment were averages and standard deviations.

## 3. Results and Discussion

### 3.1 The simulation result of temperature in GSD

Based on the simulations using the CFD software, the temperature inside the digesters was calculated. The simulation results showed that the average temperature in the GSD was influenced by the heat generated by solar radiation. The effect of high average temperatures may result in higher biogas production efficiency of the TSAD. During the day, there may be times when the temperature of the substance in the digester is too high, which will exceed the temperature in the mesophilic range (30-40°C). Therefore, the researchers installed fans on the side of the GSD with a temperature control system to keep the temperature from exceeding a certain threshold. Fans were responsible for dissipating heat from the GSD, reducing the temperature inside the dome. The results of the CFD simulation were compared for GSD-integrated and GSD-free systems, as shown in Figure 9. The

duration of the mathematical simulation of the system started at 7:00 AM on day 1 and ended at 7:00 AM on day 3. The simulation results showed that the average temperature of the GSD-integrated system was higher than the GSD-free system. This was because the GSD-free system (traditional system) was not designed to receive solar radiation directly. It was different from the GSD-integrated system, which had a parabola shape that allowed solar radiation to penetrate the dome surface resulting in a higher average temperature inside the GSD system more than the GSD-free system. In addition, from the graph, the average temperature on the 2<sup>nd</sup> day was higher than the first day. This was because there was heat accumulation in the system at the end of the first day resulting in an increased system temperature on the 2<sup>nd</sup> day. The highest system temperature was 44.3°C during the day and the lowest temperature was 32°C at night. In practice, the system was equipped with a temperature control unit to maintain the temperature within a preset value of 40°C.

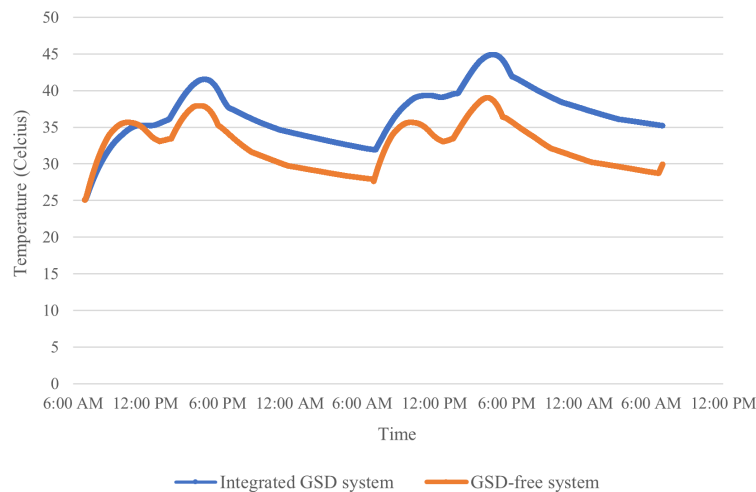


**Figure 9.** Temperature variation of GSD-integrated and GSD-free system

The results of simulations using CFD techniques are shown in Figure 10 in the form of temperature contours of the substance in the digester for each fermentation period. The results of the TSAD integrated with the GSD system and the GSD-free system, were compared. At the start of the system, the temperature value was kept low, but as the system progressed, the temperature gradually increased due to the influence of solar radiation. After that, it gradually decreased during the night. The average temperature on the 2<sup>nd</sup> day was slightly higher than the 1<sup>st</sup> day since there was no accumulated heat in the digesters on the first day. In addition, the temperature contour of the GSD-integrated system had a darker color than the GSD-free system (Figure 10). This was because the temperature levels of the substance in the digester of the GSD-integrated system was higher than those of the GSD-free system.

### 3.2 The effect of temperature on the amount of biogas produced

#### 3.2.1 Temperature variation in the digestion system

The research was conducted in September at the Waste Management and Environment Center, Kalasin University, Muang District, Kalasin Province. Generally, during September, which marks the end of the rainy season in Thailand, there is less sunlight. The research team measured and

recorded the temperature in the digester and the average daily temperature values, which are shown in Figure 11. Table 1 shows a comparison of the average digester temperatures of the GSD-integrated system and the GSD-free system, which were 37.3°C and 32.1°C, respectively. The temperature of the GSD-integrated system was then 5.2°C higher than that of the GSD-free system, which was a 16.2% increase. This was due to the GSD system accumulating a significant amount of heat produced by solar energy during the day. As a result, the GSD system's temperature can reach 40°C. Furthermore, the accumulated heat in the system is transferred to the environment during the night, causing the system temperature to rapidly fall. However, the GSD-integrated system has the advantage of being able to retain heat and prevent heat loss from the system better than the GSD-free system.

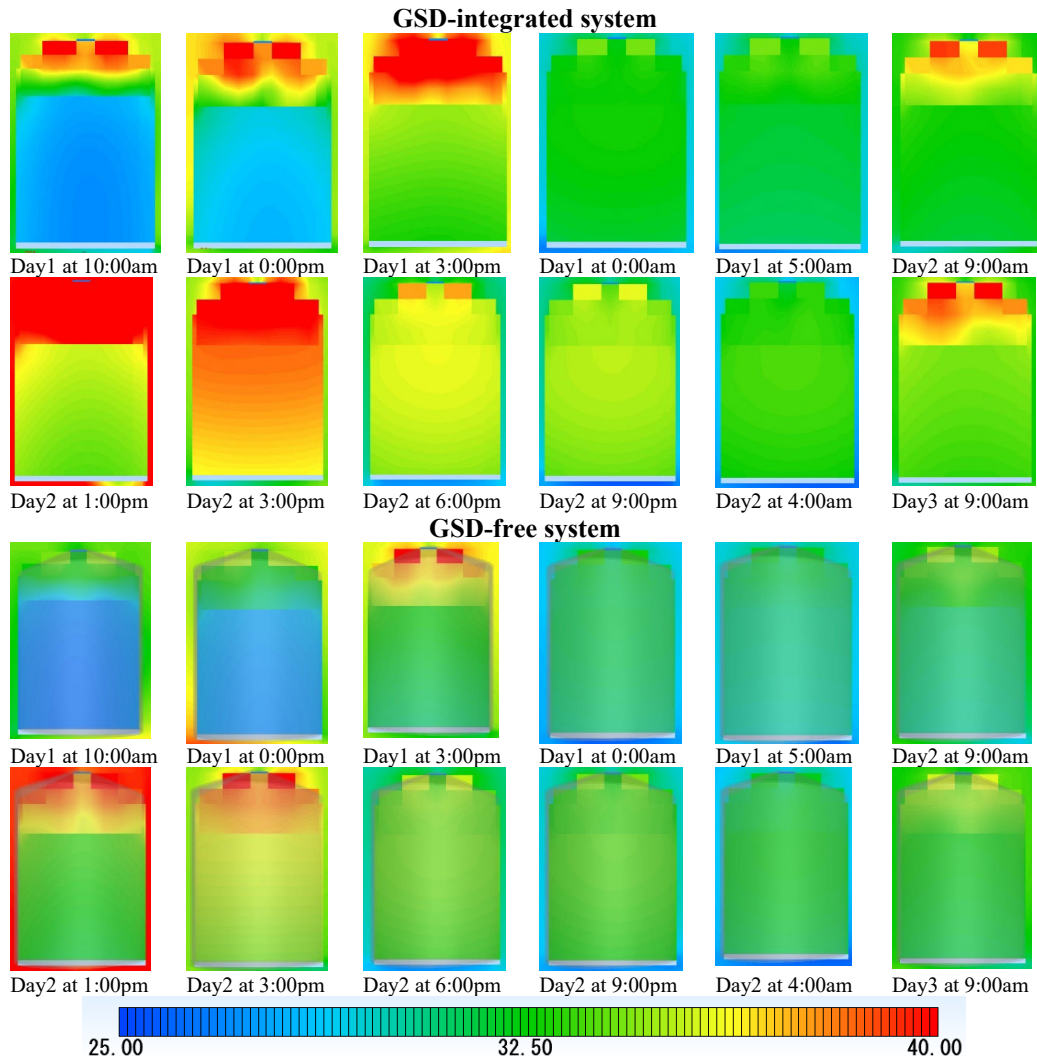


**Figure 10.** The temperature contours of the digester for each time

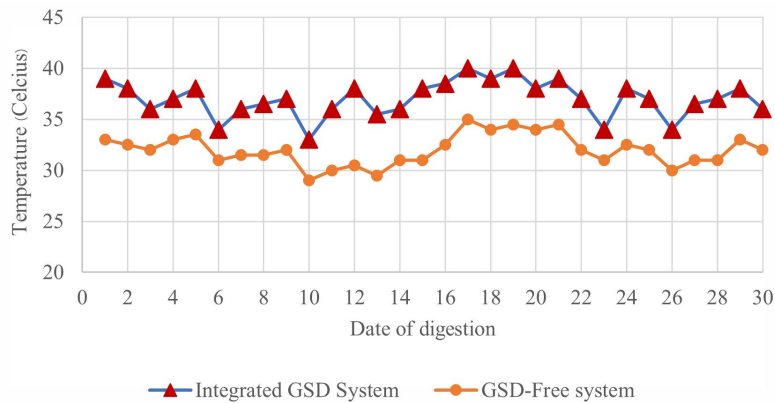


**Figure 11.** The daily temperature in the gas digester of the GSD-integrated system

**Table 1.** Temperature comparison of digester in conventional system and integrated system (GSD)

Digestion System	Conventional System	GSD-integrated System	Temperature Difference	% Change
Average Temperature (°C)	32.1	37.3	5.2	+16.2%

### 3.2.2 TSAD experiment results

In this study, biogas was produced in the conventional GSD-free system and in the GSD-integrated system. The digestion period was 30 days, and the food waste (FW) feeding rate was 3.33 L/day. Figure 12 illustrates the results of the system parameter measurements. The results of the GSD-integrated and GSD-free systems based on pH, VFA, TS, VS, SS, and COD values were compared. The samples were taken both in the methane sub-tank and before filling into the acid tank. The experiment showed that the pH variations were within the range in which methane-producing microorganisms can survive, and further were in the range appropriate for degradation in anaerobic environments because biogas production usually happens at pH 6.6-7.6 [15]. In the case of TS, VS, and SS, the results showed that the GSD-integrated system had lower TS, VS, and SS values than the GSD-free system. This may be because the GSD-integrated system's increased temperatures had the effect of accelerating the biodegradation of organic compounds into small molecules, which could be more effectively decomposed into inorganic compounds. In terms of the COD and VFA values, when comparing the two systems, it was found that the values obtained for the GSD-integrated system were greater than those obtained from the GSD-free system. This was due to the possibility that higher temperatures allowed microorganisms to consume more organic matters that were difficult to decompose. As a result, cell walls and tissue layers were damaged, resulting in an increase in the amount of dissolved substances and volatile acid content. According to Table 2, the average pH values in GSD-integrated and GSD-free systems were  $6.89 \pm 0.67$  and  $7.05 \pm 0.84$ , respectively. The average COD values were  $20.37 \pm 0.62$  g/L and  $19.61 \pm 1.10$  g/L, respectively. The average TS values were  $57.13 \pm 1.05$  g/L and  $58.04 \pm 0.85$  g/L, respectively. The average VS values were  $19.73 \pm 0.42$  g/L and  $21.82 \pm 1.28$  g/L, respectively. The average SS values were  $14.36 \pm 0.46$  g/L and  $16.30 \pm 1.32$  g/L, respectively. Finally, the average VFA values were  $0.344 \pm 0.059$  g/L and  $0.336 \pm 0.037$  g/L, respectively.

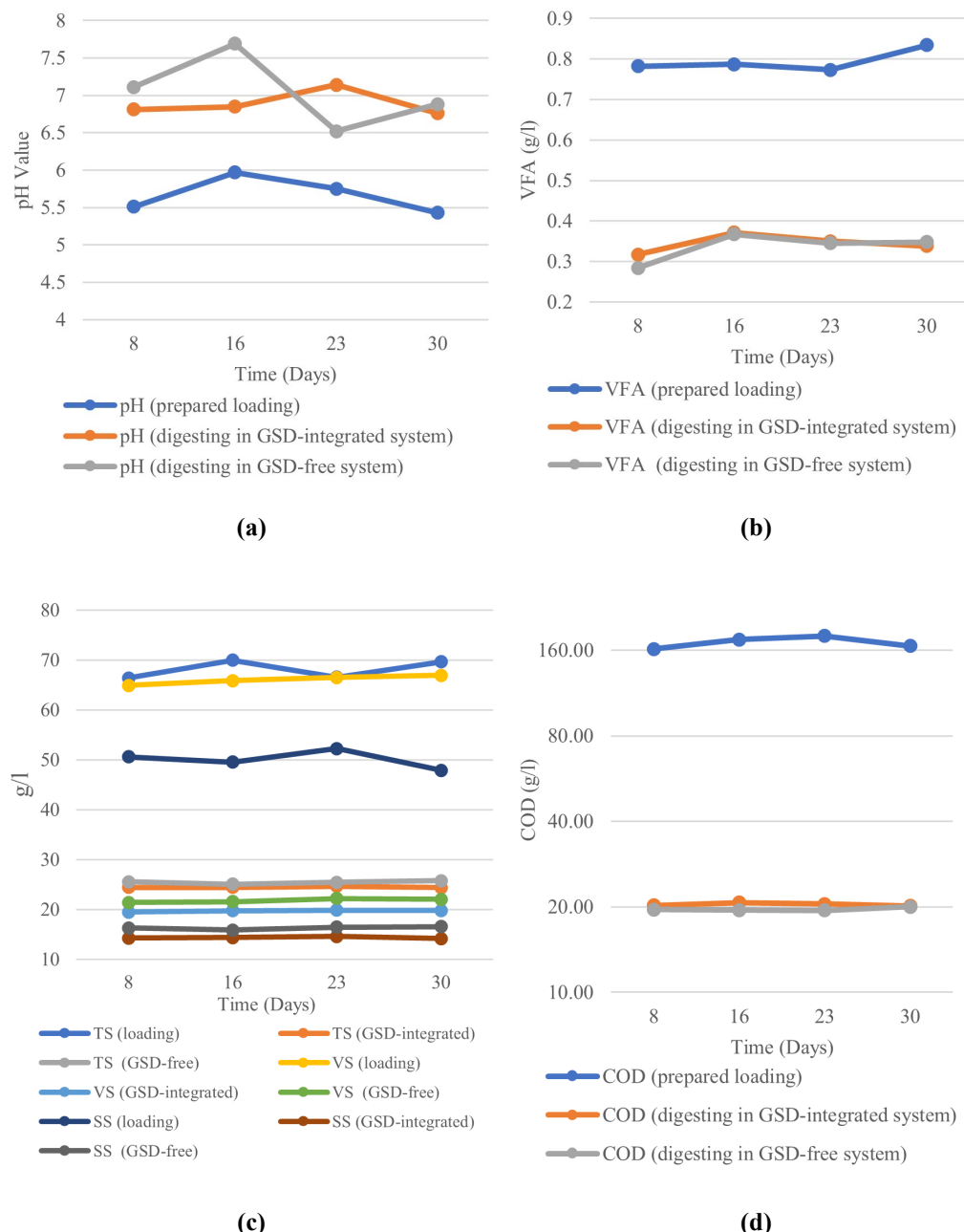


**Figure 12.** Change of organic waste pH, TS, VS, SS, VFA, COD during the test

**Table 2.** Characteristics of organic waste in the digestors

Value	Prepared Loading Substance	Substance in Digestor (GSD-integrated System)	Substance in Digestor (GSD-free System)
pH	5.66±0.34	6.89±0.67	7.05±0.84
Cod (g/L)	170.27±11.32	20.37±0.62	19.61±1.10
TS (g/L)	68.15±2.25	24.48±1.05	25.47±0.85
VS (g/L)	66.05±2.21	19.73±0.42	21.82±1.28
SS (g/L)	50.07±2.31	14.36±0.46	16.30±1.32
VFA (g/L)	0.794±0.045	0.344±0.059	0.336±0.037

The experimental results of biogas production rate are shown in Figure 13a. The digestion period from the beginning to the 7<sup>th</sup> day showed that the biogas production rate in the system increased due to the bacteria in the system increasing until it reached a steady state. After the 7<sup>th</sup> day, the system tended to produce a relatively stable biogas production rate. The average daily biogas production rate in the conventional GSD-free and GSD-integrated systems were 0.518 L/g-VS and 0.62 L/g-VS, respectively.

The relationship between the rate of biogas production and the temperature of the fermentation is shown in Figure 13b. As shown in the graph, the trendline appears to be linear for both systems. The rate of biogas production increased with increasing system temperature. The correlation values for the two variables in the GSD-integrated and GSD-free systems were 0.786 and 0.806, respectively.

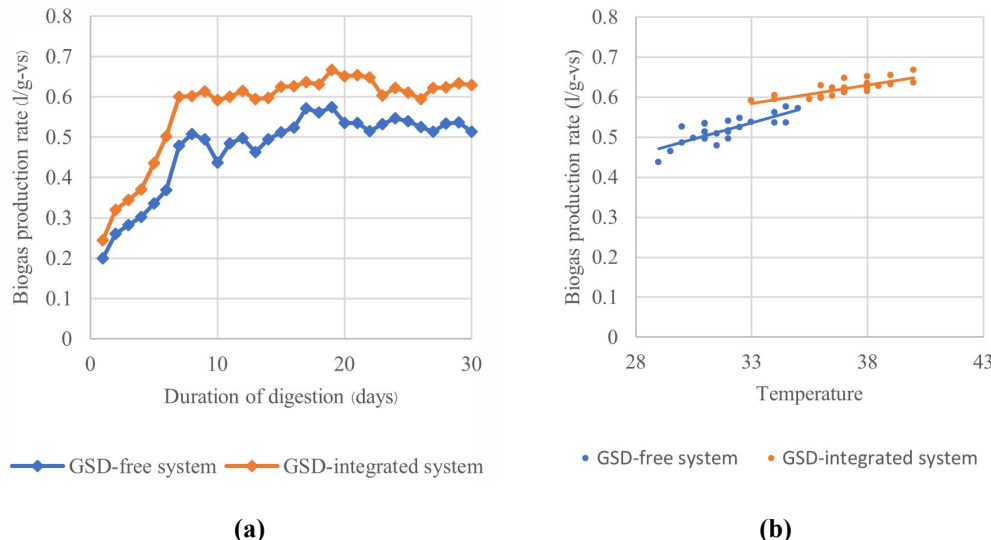
**Figure 13.** Comparison of biogas production rate for GSD-free and GSD-integrated systems

Table 3 is a comparison of the results of biogas production rates by digestion technique, type of waste, and different digestion conditions. By comparing the results of this study, the GSD-integrated system provided very high rates of biogas production. This was better than the GSD-free system and differed little from the results of Paudel *et al.* [16]. In their research, it was observed that

**Table 3** The average daily biogas production rates

Type and Condition [References]	Type of Waste	Temperature	HRT1/ HRT2	OLR	Biogas Production Rate (L/g VS)
CSTR/CSTR Continuous/ Continuous Paudel <i>et al.</i> [16]	FW and wastewater	37±1/37±1	8 h/20 d	106 g-VS.d <sup>-1</sup> /L 1.24 g-VS.d <sup>-1</sup> /L	728 mL /g-VS
CSTR/CSTR Semi-continuous/ Continuous Pavan <i>et al.</i> [17]	MSW	34.6/54.9	4.6 d/7.7 d	16.4 g-VS.d <sup>-1</sup> /L 7.4 g-VS.d <sup>-1</sup> /L	560 mL /g-TVS
CSTR/AB Semi- continuous/Semi- continuous Chu <i>et al.</i> [18]	FW	55.0/35.0	1.3 d/5.0 d	38.4 g-VS.d <sup>-1</sup> /L 6.6 g-VS.d <sup>-1</sup> /L	747 mL/g-VS
CSTR/CSTR Continuous/ Continuous Salsali <i>et al.</i> [19]	Sludge	35/35	5 d/10 d	6.4–7.6 g-VS.d <sup>-1</sup> /L 3.2–3.8 g-VS.d <sup>-1</sup> /L	302–360mL/g- VS
GSD-Free system (This research)	FW	32±1	24 d	2.75±0.12 g-VS.d <sup>-1</sup> /L	518±3.6 mL/g- VS
GSD-integrated system (This research)	FW	37±1	24 d	2.75±0.12 g-VS.d <sup>-1</sup> /L	620±5.8 mL/g- VS

the digestion temperature was 37±1°C, which was close to the finding in this research. In their work, the effect of digestion was slightly different, and the use of wastewater contributed to better digestion efficiency.

In the research of Pavan *et al.* [17] and Chu *et al.* [18], although the experiments were conducted in a thermophilic environment, only one stage of fermentation was performed. The other stage was carried out at a temperature in the mesophilic range, resulting in biogas production not being as high as expected. Therefore, systems with similar temperature environments for both stages of digestion seem to be optimal for digestion. Additionally, sludge-based digestion appears to provide lower gas production rates than FW-based digestion.

#### 4. Conclusions

The TSAD system integrated with GSD was studied. Initially, daily temperature changes due to the influence of solar radiation inside the digester were investigated. This was simulated with CFD techniques using computer software. The simulation results showed that the digester temperature range was close to the mesophilic range, which was suitable for use in TSAD systems.

In the comparison of the biogas production rates between TSAD integrated with GSD and conventional GSD-free systems, it was found that from the start of the experiment until the 8<sup>th</sup> day, the biogas production rate increased. This was due to the increased number of bacteria in the system resulting in catalysts of biogas production. After the 8<sup>th</sup> day, the system entered a state of relatively stable biogas production. The average biogas production rates of the GSD-free system and GSD-integrated system were 0.518 L/g-VS and 0.62 L/g-VS, respectively. It can be concluded that the

GSD system compared to the conventional system provided a higher rate of biogas production because the average temperature was higher than the conventional system. A high system average temperature can accelerate the digestion reaction of organic waste and increase the rate of biogas generation. The results of the average daily biogas production rate of the GSD system compared to the conventional system showed an increase of 19.69%

Because it is powered by the sun, the TSAD integrated with GSD system has an advantage over conventional systems in that it can generate a higher overall system temperature without the need for electrical power. This experimental system's usability constraint is climatic change, where the system runs optimally during sunlight. However, if it rains or is cloudy in the daytime, the rate of biogas production may be affected. For future study, the wastewater in digestion with FW and cow manure to optimize the TSAD GSD-integrated fermentation for higher biogas production will be conducted. In addition, this system is also planned to be used at the community level in order to increase the biogas production because the system is cost-efficient and simple-to-install.

## 5. Acknowledgements

The authors wish to thank the support of the Faculty of Engineering and Industrial Technology of Kalasin University.

## References

- [1] Demirel, B. and Yenigun, O., 2002. Two-phase anaerobic digestion processes: a review. *Journal of Chemical Technology and Biotechnology*, 77, 743-755.
- [2] Ahn, J.H. and Forster, C.F., 2002. The effect of temperature variations on the performance of mesophilic and thermophilic anaerobic filters treating a simulated papermill wastewater. *Process Biochemistry*, 37, 589-594.
- [3] Moestedt, J., Rönnberg, J. and Nordell, E., 2017. The effect of different mesophilic temperatures during anaerobic digestion of sludge on the overall performance of a WWTP in Sweden. *Water Science and Technology*, 76(12), 3213-3219.
- [4] Thai Meteorological Department, 2020. *Thailand Annual Weather Summary*. [online] Available at: <https://www.tmd.go.th/climate/climate.php?FileID=5>.
- [5] Janjai, S., 2012. A greenhouse type solar dryer for small-scale dried food industries: Development and dissemination. *International Journal of Energy and Environment*, 3(3), 383-398.
- [6] Iqbal, M., 1983. *An Introduction to Solar Radiation*. Toronto: Academic Press.
- [7] Kasten, F. and Young, T., 1989. Revised optical air mass tables and approximation formula. *Applied Optics*, 28, 4735-4738.
- [8] Thevenard, D. and Gueymard, C., 2010. Updating the ASHRAE climatic data for design and standards. *ASHRAE Transactions*, 116(2), 444-459.
- [9] Owen, M.S. and Kennedy, H.E., 2009. *ASHRAE Handbook: Fundamentals*. SI ed. Atlanta: American Society of Heating, Refrigerating and Air-conditioning Engineers, Inc.
- [10] Stephenson, D.G., 1965. Equations for solar heat gain through windows. *Solar Energy*, 9(2), 81-86.
- [11] Threlkeld, J.L., 1963. Solar irradiation of surfaces on clear days. *ASHRAE Transactions*, 69, 24-36.

---

- [12] Janjai, S., Intawee, P., Kaewkiew, J., Sritus, C. and Khamvongsa, V., 2011. A large-scale solar greenhouse dryer using polycarbonate cover: Modeling and testing in a tropical environment of Lao People's Democratic Republic. *Renewable Energy*, 36, 1053-1062.
- [13] Srisowmeya, G., Chakravarthy, M. and Devi, G.N., 2019. Critical considerations in two-stage anaerobic digestion of food waste – A review. *Renewable and Sustainable Energy Reviews*, 119, DOI: 10.1016/j.rser.2019.109587.
- [14] Van, D.P., Fujiwara, T., Tho, B.L., Toan, P.P.S. and Minh, G.H., 2019. A review of anaerobic digestion systems for biodegradable waste: Configurations, operating parameters, and current trends. *Environmental Engineering Research*, 25(1), 1-17.
- [15] Ghaly, A. and Ben-Hassan, R., 1989. Continuous production of biogas from dairy manure using an innovative no-mix reactor. *Applied Biochemistry and Biotechnology*, 20, 541-559.
- [16] Paudel, S., Kang, Y., Yoo, Y.S. and Seo, G.T., 2017. Effect of volumetric organic loading rate (OLR) on H<sub>2</sub> and CH<sub>4</sub> production by two-stage anaerobic co-digestion of food waste and brown water. *Waste Management*, 61, 484-493.
- [17] Pavan, P., Battistoni, P., Cecchi, F. and Mata-Alvarez, J., 2000. Two-phase anaerobic digestion of source sorted OFMSW (organic fraction of municipal solid waste): performance and kinetic study. *Water Science and Technology*, 41, 111-118.
- [18] Chu, C.F., Li, Y.Y., Xu, K.Q., Ebie, Y., Inamori, Y. and Kong, H.N., 2008. A pH- and temperature-phased two-stage process for hydrogen and methane production from food waste. *International Journal of Hydrogen Energy*, 33, 4739-4746.
- [19] Salsali, H., Parker, W. and Sattar, S., 2005. Influence of staged operation of mesophilic anaerobic digestion on microbial reduction. *Proceedings of the Water Environment Federation*, 11, 4571-4586.